CHEMICAL ENGINEERING TRANSACTIONS
VOL. 87, 2021
A publication of AIDIC
The Italian Association of Chemical Engineering
Online at www.cetjournal.it
Guest Editors: Laura Piazza, Mauro Moresi, Francesco Donsì

ISBN 978-88-95608-85-3; **ISSN** 2283-9216

Non-Isothermal Moving-Boundary Model for Food Drying

Antonio Brasiello *, Claudia Venditti, Alessandra Adrover

Dipartimento di Ingegneria Chimica Materiali Ambiente, Università degli Studi di Roma "La Sapienza", via Eudossiana 18 00184 Roma, Italy
antonio.brasiello@uniroma1.it

Mathematical modeling of food drying represents a key research topic. Drying is one of the most used processes in food technology. It is a complex process in which water concentration changes are very often associated with volume and structural variations of materials. This phenomenon, known as shrinkage, limits the possibility of using classical transport models to obtain reliable results for drying process analysis and control. Drying is intrinsically a non-isothermal process, even when it is performed under "isothermal" conditions, meaning when the air temperature in the drying chamber is kept constant. Indeed, thermal inertial of food samples, as well as thermal effects due to water evaporation at the sample boundary, must be necessarily taken into account for a deep understanding of the process and a reliable estimate of the effective water diffusivity. Moreover, in many practical applications, food drying takes place in non-isothermal conditions. The isothermal moving-boundary model for food dehydration and shrinkage, recently proposed by Adrover et al. (2019b,c), is here improved to account for thermal effects. A convection-diffusion heat transport equation, accounting for heat transfer, water evaporation, and shrinkage at the sample surface, is added to the convection-diffusion water transport equation. Experimental dehydration curves, in continuous and intermittent conditions, are accurately predicted by the model with an effective water diffusivity $D_{\text{eff}}(T)$ depending exclusively on the local temperature. The non-isothermal model is successfully applied to experimental data of continuous and intermittent drying of Guava slices, reported by Chua et al. 2000a.

1. Introduction

Food drying processes are often carried out in non-isothermal conditions. In the case of natural drying, for example, temperature strongly depends on the environmental conditions of the production sites (climate, day-night temperature range, and seasonal variations). In some cases, natural drying ensures added value to the final products from the point of view of organoleptic properties deeply influenced by the specific production area. In many other cases, natural drying is chosen only for its economic advantage. In such cases, the main drawback stands in being the characteristics of the final products highly heterogeneous.
Intermittent drying is a technical solution providing the advantage of increasing drying efficiency and product quality, assuring uniform characteristics, through the suitable choice of the optimal temperature and humidity profiles during the process. Moreover, several literature papers (see Yang et al., 2013 and reference therein) highlight the possibility of reducing color degradation through intermittent drying.
The possibility of optimizing process conduction is directly connected to the availability of theoretical models that provide the technical tools for the process evolution analysis as conditions vary.
Mathematical model development in this field is not an easy task due to the complexity of the materials involved. During drying, foods undergo structural and volume variations not predictable with the classic mathematical models (diffusive models based on Fick's law of diffusion). The phenomenon is known as shrinkage. Two approaches are available in literature: in the first, based on mechanical equations for deformable bodies, shrinkage is taken into account through constitutive equations for stress-deformation tensor, depending on the internal structure of the material and process variables (as in the model of Curcio and Aversa (2014) or the pore-mechanical model of Dhall and Datta (2011)); the second approach, borrowed from polymer science (Papanu et al., 1989; Tu and Ouano, 1977), is the moving-boundary model developed by Adrover et al. (2019b). In this case, shrinkage is taken into account through a suitable parameter, describing the point-wise shrinkage velocity evolution as a function of the local water content gradient. Adrover

et al. (2019c) have shown that such a parameter can be easily derived from the experimental diagram of volume vs. total water content evolution of drying sample. The moving-boundary model has been recently extended to account for non-isothermal effects, see Adrover et al., 2020. Thermal effects are modeled through the introduction of a convection-diffusion heat transport equation, accounting for sample shrinkage, heat transfer, and water evaporation at the sample surface. When the spatio-temporal evolution of the temperature field is properly accounted for, the experimental dehydration curves, in continuous and intermittent conditions, can be accurately predicted by the moving-boundary model with an effective water diffusivity $D_{\text{eff}}(T)$ depending exclusively on the local temperature.
In this paper, the non-isothermal model is applied to a case of non-isothermal drying available in literature (Chua et al, 2000a,b). The interesting papers by Chua et al. (2000a,b) report a set of experimental data of continuous and intermittent drying of Guava slices in which air temperature and relative humidity vary cyclically in a climatic chamber. Guavas are characterized by high initial moisture content and exhibit a large ideal shrinkage. The model, applied to continuous dehydration experiments, allows for a reliable estimate of the effective water diffusivity, which is the only unknown parameter that enters the non-isothermal model. All the other parameters have been estimated from independent measurements (e.g. water adsorption isotherms) and reliable correlations for heat and mass transfer coefficients. The model is subsequently successfully applied, in a fully predictive way, to capture all the salient features of the intermittent drying experiments, highlighting the importance of accounting for thermal inertial of the food sample as well as thermal effects of water evaporation at the sample boundary for a correct description of the drying process.

2. Drying experiments

Experimental data of continuous and intermittent dehydration of Guava fruit (Psidium Guajava) are taken from the paper of Chua et al., 2000a. Guava samples were dried in a two-stage heat pump dryer in which the drying chamber temperature and humidity profiles are imposed through PID controllers. Fresh guava fruits were skinned, peeled, and cut to obtain square slices with thickness $H_0 = 3\ \text{mm}$ and side $L_0 = 30\text{mm}$. Guava slices were then placed in a single layer on the dryer's tray. Details about the experimental setup can be found in the original papers of Chua et al., 2000a,b. Two types of drying experiments were considered: continuous (C), in which the air temperature and humidity were kept constant, and intermittent (I) in which square wave (period 60 min) temperature profiles where imposed, corresponding to square wave humidity profiles, since the air humidity and velocity were held constant at $\Omega = 0.0089\ \text{kg/kg}$ and $U_\infty = 2.5\ \text{m/s}$, respectively. The operating temperature and humidity for continuous experiments C25, C30 and C40 as well as the maximum and minimum values of temperature and humidity for the three intermittent experiments I25, I30, I40 are summarized in Table 1.

Table 1: Continuous and intermittent experiments.

Type	T_∞	RH_∞
C25	25°C	43.2
C30	30°C	32.5
C40	40°C	19.8
I25	30°C - 20°C	31.8 - 65.1
I30	35°C - 25°C	24.8 - 47.9
I40	40°C - 30°C	18.9 - 33.5

3. Mathematical model

The moving-boundary model developed in Adrover et al., 2020 for non-isothermal drying consists of a system of two advection-diffusion partial differential equations for mass and energy transport, coupled with an equation for the boundary evolution, the material being assumed homogeneous and isotropic.
In the one-dimensional formulation that can be adopted for Guava slices (heat and mass transport along the thickness coordinate $-\text{H}_0/2 \le \text{x} \le \text{H}_0/2$), the transport equations for the water content $c_w(x,t)$ $[\text{g water/m}^3]$ and the sample temperature $T(x,t)$ read as:

$$\frac{\partial c_w(x,t)}{\partial t} = \frac{\partial}{\partial x}\left(D_{\text{eff}}(T)\,\frac{\partial c_w}{\partial x} - v_s(x,t)\,c_w\right), \quad 0 < x < x_b(t) \tag{1}$$

$$\frac{\partial\left(\rho^p\, C_p^p\, T(x,t)\right)}{\partial t} = \frac{\partial}{\partial x}\left(k^p\,\frac{\partial T}{\partial x} - v_s(x,t)\,\rho^p\, C_p^p\, T\right), \quad 0 < x < x_b(t) \tag{2}$$

Where ρ^p is the sample density, C_p^p the specific heat at constant pressure, k^p the thermal conductivity and $D_{\text{eff}}(T)$ the effective water diffusivity. The velocity $v_s(x,t)$ is the point-wise shrinkage velocity

$$v_s(x,t) = \alpha(c_w)\frac{D_{\text{eff}}(T)}{\rho_w}\frac{\partial c_w}{\partial x}, \quad \frac{dx_b}{dt} = v_s\Big|_{x_b(t)} = \frac{D_{\text{eff}}(T_b)}{\rho_w}\alpha(c_w)\frac{\partial c_w}{\partial x}\Big|_{x_b(t)} \tag{3}$$

affecting both the heat and mass transport equations and controlling the temporal evolution of the sample surface $x_b(t)$. The shrinkage proportionality factor $\alpha(c_w)$, entering the shrinkage velocity and depending on the point-wise water content $c_w(x,t)$, is the fingerprint of the specific food material under investigation. The simplest case is that of a constant shrinkage factor, $\alpha(c_w) = \alpha_0$. Specifically, $\alpha_0 = 0$ represents the case of a rigid solid (no shrinkage), while $\alpha_0 = 1$ represents the case of ideal shrinkage, in which volume reduction corresponds exactly to the volume of water flowing outside the sample.

The two transport equations (1) and (2) are linked together and must be solved simultaneously by further enforcing the symmetry boundary conditions at $x = 0$ and the mixed boundary conditions at $x_b(t)$ also referred to as Robin or "evaporative" or third order boundary condition (da Silva et al., 2015)

$$-D_{\text{eff}}(T_b)\frac{\partial c_w}{\partial x}\Big|_{x_b} = h_m(T_{\text{av}})M_w\left(\frac{p_v(T_b)}{R_g T_b}RH_b - \frac{p_v(T_\infty)}{R_g T_\infty}RH_\infty\right) \tag{4}$$

$$-k^p\frac{\partial T}{\partial x}\Big|_{x_b} = h_T(T_{\text{av}})(T_b - T_\infty) - \lambda_v(T_b)D_{\text{eff}}(T_b)\frac{\partial c_w}{\partial x}\Big|_{x_b} \tag{5}$$

where M_w is the water molecular weight, $p_v(T)$ the saturated vapor pressure at temperature T, h_m and h_T are the mass and heat transport coefficients, RH_b and T_b the relative humidity and the temperature at the sample boundary $x_b(t)$, RH_∞ and T_∞ the air relative humidity and the temperature in the drying chamber.

The boundary condition (5) takes into account both heat transfer resistance and heat subtracted for water evaporation at the air/sample interface (Carslaw and Jaeger, 1959), $\lambda_v(T_b)$ being the heat of water evaporation evaluated at T_b.

The heat and mass transfer coefficients h_m and h_T can be evaluated from well-known correlation functions for the Sherwood (Sh) and Nusselt (Nu) numbers, specific for the sample geometry (slab) under investigation,

$$Nu(T_{\text{av}}) = 0.664\,Re^{1/2}Pr^{1/3} = \left(\frac{U_\infty L}{\nu_{\text{air}}(T_{\text{av}})}\right)^{1/2}\left(\frac{\nu_{\text{air}}(T_{\text{av}})}{D_T^{\text{air}}(T_{\text{av}})}\right)^{1/3} \tag{6}$$

$$Sh(T_{\text{av}}) = 0.664\,Re^{1/2}Sc^{1/3} = \left(\frac{U_\infty L}{\nu_{\text{air}}(T_{\text{av}})}\right)^{1/2}\left(\frac{\nu_{\text{air}}(T_{\text{av}})}{D_v^{\text{air}}(T_{\text{av}})}\right)^{1/3} \tag{7}$$

with all the physical parameters of the wet air evaluated at the average film temperature $T_{\text{av}} = (T_\infty + T_b)/2$.

All the physical parameters of the food sample, namely ρ^p, C_p^p, and k^p, are functions of the local water concentration c_w. Specifically, the sample density ρ^p is evaluated as the average of the water and solid (pulp) densities, averaged with respect to their volume fractions $\rho^p = \rho^w\,\phi_w + \rho^s(1-\phi_w)$, with $\rho^S \simeq 1.5\ \text{g/cm}^3$ for carbohydrates. The product heat capacity C_p^p is evaluated as the average of the water and solid specific heat capacity $C_p^p = C_p^w\,x_w + C_p^S\,(1-x_w)$, averaged with respect to their weight fractions $x_w = \phi_w(\rho^w/\rho^p)$. The sample thermal conductivity k^p is evaluated from a parallel model $1/k^p = \phi_w/k^w + (1-\phi_w)/k^S$ where k^w and k^S are the water and solid thermal conductivities, respectively. Since Guava fruits contain mainly water and carbohydrate (Rahman et al., 1997), the thermal conductivity k^S and the specific heat capacity C_p^S of the solid are estimated from that of carbohydrate (Becker and Fricke, 2003)

$$k^s[\text{W/(m K)}] = 2.01\times10^{-1} + 1.39\times10^{-3}T - 4.33\times10^{-6}T^2\ ,\ T[^oC] \tag{8}$$

$$C_p^s[\text{J/(g K)}] = 1.5488 + 1.9625\times10^{-3}T - 5.9399\times10^{-6}T^2\ ,\ T[^oC] \tag{9}$$

The relative humidity at the air/sample interface RH_b evolves in time because both $c_w(x_b)$ and T_b change during the course of the dehydration process. The relationship $RH_b = f(T_b, c_w)$ can be estimated from water vapor adsorption isotherms of Guava reported from (Hubinger et al., 1992). Adsorption isotherms in the range $[25^oC, 50^oC]$ are almost independent of temperature and well fitted ($R^2 = 0.999$) with the modified Anderson model (Guinè, 2009) relating the equilibrium relative humidity RH_{eq} to the equilibrium moisture content X_{eq}

$$RH_{eq}(X_{eq}) = 1 - \exp(-a\,X_{eq}^b),\ a = 3.45,\ b = 0.63,\quad X_{eq}[\text{kg w/kg dry solid}] \tag{10}$$

A latter observation regarding the shrinkage proportionality factor $\alpha(c_w)$ adopted for Guava fruits: Guavas, as pears and carrots, are characterized by very high-water content $x_w \in (80\%, 82\%)$ [g water/g product] (USDA, 2020). All fruits with high initial moisture content exhibit an almost ideal shrinkage, that implies $\alpha(c_w) = \alpha_0 = 1$ and $V_\infty/V_0 \simeq 1 - \phi_w(0)$, V_∞ being the asymptotic sample volume at the end of the dehydration process and $\phi_w(0)$ the initial water volume fraction, supposed uniform within the sample. For a slice sample with aspect ratio $AR = L_0/H_0 = 10$, shrinkage affects all the three slice dimensions, even if the most affected is the slice thickness, and the asymptotic rescaled slice thickness H_∞/H_0 can be approximately related to the asymptotic volume ratio V_∞/V_0 by the relation (Adrover et al., 2019a)

$$V_\infty/V_0 = H_\infty/H_0\,(A\,R - 1 + H_\infty/H_0)^2/A\,R^2 \tag{11}$$

This implies that an asymptotic thickness reduction $H_\infty/H_0 \simeq 1/3$ corresponds to an asymptotic volume reduction $V_\infty/V_0 \simeq 0.2$. Therefore, in a one-dimensional model of the drying process in which only thickness reduction is accounted for, it is necessary to introduce a constant shrinkage factor $\alpha_0 \simeq 0.83 < 1$ to guarantee $H_\infty/H_0 \simeq 1/3$, corresponding to the ideal volume shrinkage, and therefore to have a correct estimate of the diffusional lengths along the principal transport/shrinkage direction.

4. Results and discussion

The only parameter, entering the non-isothermal model, that needs to be estimated is the effective water diffusivity $D_{\text{eff}}(T)$ and its dependence on temperature T. $D_{\text{eff}}(T)$ can be estimated from continuous dehydration curves C25, C30 and C40, reported in Figure 1A, showing the temporal decay of the moisture content $X(t)$ [kg w/kg dry basis] rescaled onto the initial moisture content X_0, for the three temperatures $T_\infty = 25, 30, 40^o C$.

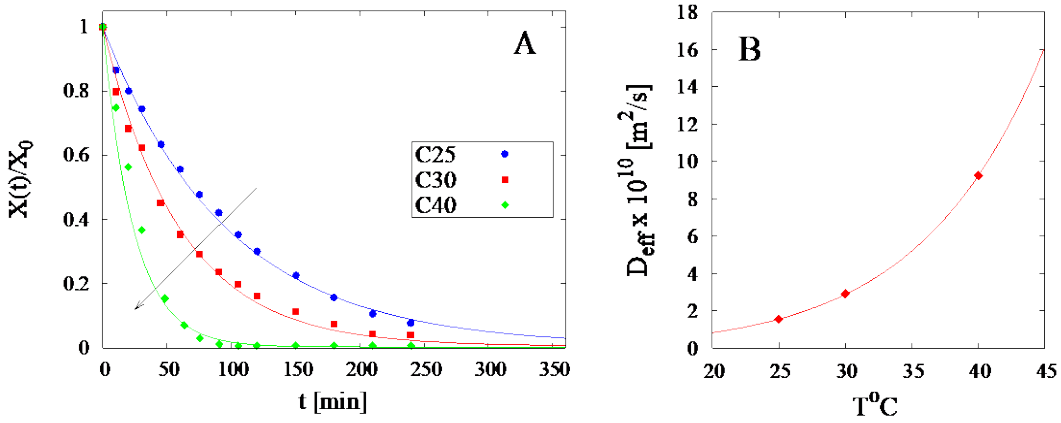

Figure 1. A) Rescaled moisture ratio vs time for the three continuous drying experiments at T=25, 30, 40°C. Continuous lines represent model predictions with the effective water diffusion coefficient $D_{\text{eff}}(T)$ reported in Figure B.

Continuous lines in Figure 1A represent best-fit non-isothermal model curves obtained with the best-fitted Arrhenius-type curve for the effective water diffusivity $D_{\text{eff}}(T)$

$$D_{\text{hii}}(T)\,[\text{p}^2/\text{v}] = D_0\text{h}\{\text{s}(-E/RT) \quad D_0 = \text{h}\{\text{s}(14.63)\,[\text{p}^2/\text{v}] \quad E/R = 11095[K] \tag{12}$$

reported in figure 1B. It can be observed that the estimated effective water diffusivity is highly sensitive to temperature as it exhibits a significant increase with temperature (Table 2.). These values of the water diffusivity are in agreement with those of other vegetables and fruits with high initial moisture ratio, although it has to be pointed out that a one-dimensional model, like the one adopted, tends to overestimate the effective diffusivity (Adrover et al., 2019a).

Table 2: Estimated effective water diffusivity D_{eff}.

T [°C]	D_{eff} [m^2/s]
25	1.557×10^{-10}
30	2.877×10^{-10}
40	9.258×10^{-10}

The estimate of $D_{\text{eff}}(T)$ from continuous drying experiments permits to verify the potentialities of the non-isothermal model by comparing experimental intermittent dehydration curves I25, I30 and I40 with model predictions (with no adjustable parameters) as shown in Figure 2.

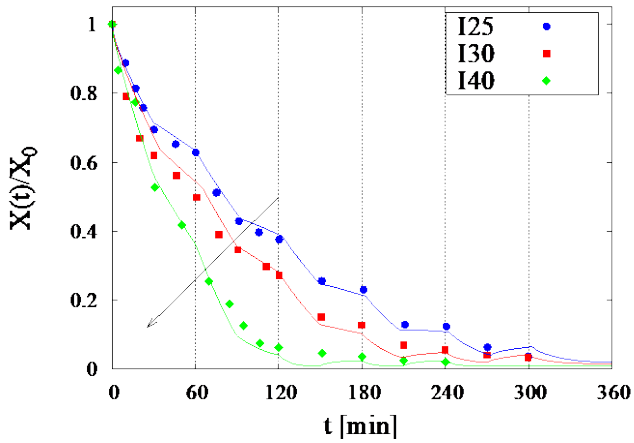

Figure 2: Model predictions of the three intermittent experiments (square wave, $\Delta T = 10^oC$, time period 60 min). Arrow indicates increasing values of the average processing temperature ($25, 30, 40^oC$, respectively).

It can be clearly observed the excellent capability of the model to follow accurately the step changes in the operating air and relative humidity conditions, by perfectly reproducing the periodic sudden changes in the slope of the curve for the rescaled moisture content $X(t)/X_0$. The model allows us to estimate the spatio-temporal evolution of all the basic quantities controlling the drying process. As an instance, Figure 3A-D show the time-behavior of the rescaled slab thickness (A), temperature (B) and relative humidity (C) at the air/sample interface as well as the heat and mass transfer coefficients (D) for the case I25. In Figure 3B it can be observed that the boundary temperature exhibits a sudden decrease at the beginning of the drying process induced by water surface evaporation. Moreover, the Guava slice has a significant thermal inertia so that the boundary temperature needs at least five periods to follow closely the square-wave air temperature.

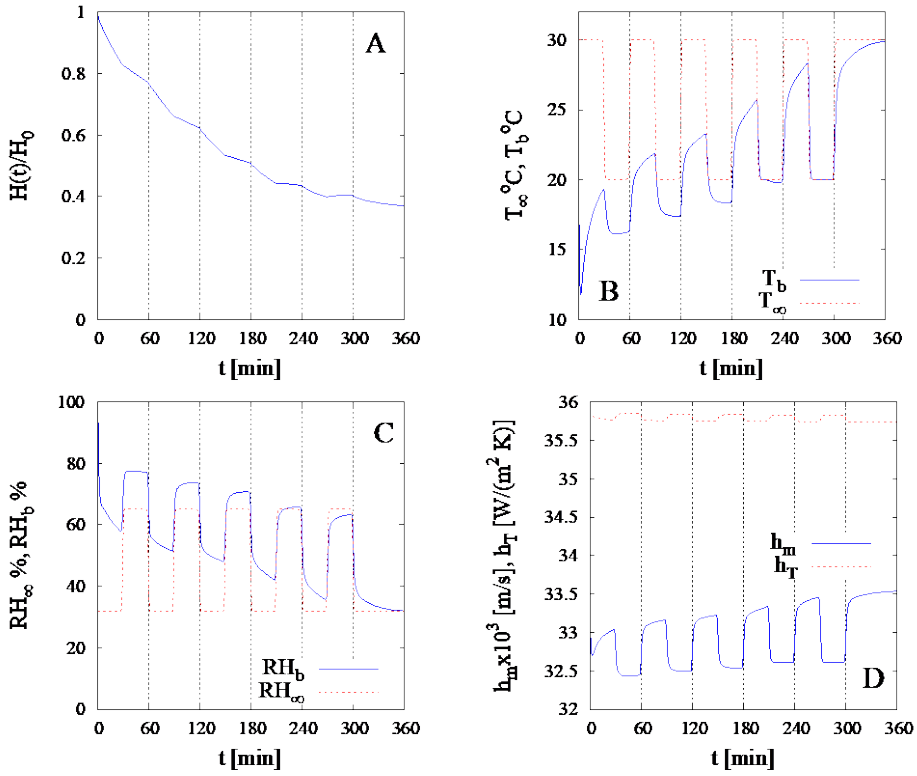

Figure 3. Model predictions of the I25 intermittent experiment (square wave, time period 60 min).

A similar observation can be done for the boundary relative humidity (see Figure 3C). Specifically, it can be observed that partial rehydration of the sample may occur when the moisture content is low. These effects are extremely important and must be accounted for when degradation kinetics of nutrients and vitamins are investigated. In this context, a reliable estimate of the internal sample temperature is extremely useful to optimize intermittent dehydration protocols to obtain low water activity while keeping significant amounts of vitamins, e.g. ascorbic acid.

Conclusions

The one-dimensional non-isothermal formulation of the moving-boundary model for food dehydration, recently proposed by Adrover et al. (2019 b,c) is here applied for the case of Guava slices. The model accounts for sample shrinkage via the introduction of the pointwise shrinkage velocity dependent on the local volumetric water flux. A suitable convection-diffusion heat transport equation, affected by sample shrinkage, heat transfer, and water evaporation at the sample surface, is added to the convection-diffusion transport equation for water concentration. The advantage of the model lies in the possibility of obtaining reliable data without huge experimental efforts. The excellent predictive capability of the non-isothermal model makes it a useful tool for non-isothermal process optimization and control at both laboratory and industrial scales.

References

Adrover A., Brasiello A., 2019a, A Moving Boundary Model for Isothermal Drying and Shrinkage of Chayote Discoid Samples: Comparison between the Fully Analytical and the Shortcut Numerical Approaches, International Journal of Chemical Engineering, 2019, 3926897.

Adrover A., Brasiello A., Ponso G., 2019b, A moving boundary model for food isothermal drying and shrinkage: General setting, Journal of Food Engineering, 244, 178-191.

Adrover A., Brasiello A., Ponso G., 2019c, A moving boundary model for food isothermal drying and shrinkage: A shortcut numerical method for estimating the shrinkage factor, Journal of Food Engineering, 244, 212-219.

Adrover A., Venditti C., Brasiello A., 2020, A Non-Isothermal Moving-Boundary Model for Continuous and Intermittent Drying of Pears, Foods, 9, 1577.

Becker B., Fricke B., 2003, Freezing Principles. In Encyclopedia of Food Sciences and Nutrition, 2nd ed.;

Caballero, B., Ed.; Academic Press, Oxford, UK, 2706–2711.

Carslaw H., Jaeger J., 1959, Conduction of Heat in Solids, Oxford University Press, Oxford, UK.

Chua K.J., Mujumdar A.S., Chou S.K., Hawlander M.N.A., Ho J.C., 2000b, Convective drying of banana, guava and potato pieces: effect of cyclical variations of air temperature on drying kinetics and color change, 18, 907-936.

Chua K.J., Chou S.K., Ho J.C., Mujumdar A.S., Hawlander M.N.A., 2000a, Cyclic air temperature drying of guava pieces: effects on moisture and ascorbic acid contents, Trans IChemE, 78, 72-78.

Curcio S., Aversa M., 2014, Influence of shrinkage on convective drying of fresh vegetables: A theoretical model, Journal of Food Engineering, 123, 36-49.

da Silva W.P., Rodrigues A.F., e Silva C.M.D.P.S., de Castro D.S., Gomes J.P., 2015, Comparison between continuous and intermittent drying of whole bananas using empirical and diffusion models to describe the processes, Journal of Food Engineering, 166, 230-236.

Dhall A., Datta A., 2011, Transport in deformable food materials: A poromechanics approach, Chemical Engineering Science, 66, 6482-6497.

Guin‡ R.P.F., 2009, Sorption isotherms of pears using different models, International Journal of fruit science, 9, 11–22.

Hubinger M., Menegalli F.C., Aguerre R.J., Suarez C., 1992, Water Vapor Adsorption Isotherms of Guava, Mango and Pineapple, Journal of Food Science, 57, 1405-1407.

Papanu J., Soane (Soong) D., Bell A., Hess D., 1989, Transport models for swelling and dissolution of thin polymer films, Journal of Applied Polymer Science, 38, 859-885.

Rahman M.S., Chen X.D., Perera C.O., 1997, An improved thermal conductivity prediction model for fruits and vegetables as a function of temperature, water content and porosity, Journal of Food Engineering, 31, 163-170.

Tu Y. O., Ouano A.C., 1977, Model for the kinematics of polymer dissolution, IBM Journal of Research and Development, 21, 131-142.

USDA, 2020, Food Composition Databases, Department of Agriculture, <https:// ndb.nal.usda.gov/ndb> (9/18/2020).

Yang Z., Zhu E., Zhu Z., Wang J., Li S., 2013, A comparative study on intermittent heat pump drying process of Chinese cabbage (Brassica Campestris L. SSP) seeds, Food and Bioproducts Processing, 91, 381-388.